TUNING NEGATIVE DIFFERENTIAL RESISTANCE IN A SINGLE MOLECULE TRANSISTOR: DESIGNS OF LOGIC GATES AND EFFECTS OF VARIOUS OXYGEN- AND HYDROGEN-INDUCED DEFECTS

A. NASRI[a*], A. BOUBAKER[a], B. HAFSI[b], W. KHALDI[a], A. KALBOUSSI[a]
[a]University of Monastir, Microelectronics and Instrumentation Laboratory,
Avenue de l' Environment -5019, Monastir, Tunisia
[b] CNRS, Centrale Lille, ISEN, Univ. Valenciennes, UMR 8520-IEMN Univ.
Lille Lille France

In this paper, a theoretical study of Single Molecule Transistor (SMT) operating as a molecular field effect transistor (MFET) has been presented. We have applied the density functional theory (DFT) in conjugation with the non-equilibrium green's function (NEGF) formalism on a pentacene device in order to acquire the I–V characteristics. The bias voltage influence on the I-V curves of the MFET was studied using MATLAB simulator. A good agreement with numerical results was found. When applied different gate voltage, a negative differential resistance (NDR) behaviors are observed almost at the same source-drain voltage. We demonstrate the application of using a single pentacene molecular FET to realize five basic logic gates with just one MFET. For the first time, we have investigated the electrical properties of a pentacene-based Single Electron Transistor (MSET) using Atomistix ToolKit (ATK) a set of atomic-scale simulators, which can determine properties of nano-scale systems. We confirmed Coulomb blockade phenomena in this molecular device and its role to obtain the NDR. Finally, the effects of various oxygen- and hydrogen-induced defect have been also considered. The NDR effect, the dependence of the defects and the coulomb Staircase state has been outlined.

1. Introduction

Recently, organic semiconductors have generated significant interest in the academic community and scientific research owing to their low cost and flexibility properties. Especially, a large effort of these research activities has focused on molecular electronics to realize devices such as organic flexible displays [1], organic light-emitting diodes (OLED) [2-3] ,solar cells [4], molecular sensors [5], Optoelectronic Devices [6] molecular junction [7], gate logic [8] and molecular memory devices [9]. Combining novel semiconducting electronic properties, these molecular devices can be manufactured with different simplified processes, which lead to reduced sizes, low power consumption and high speed [10].

The electron transport mechanisms have an important interest in the development of molecular organic devices and in the optimization of their characteristics and models. Some research in physical modeling have been directed toward extending these studies to chemically nanostructures, such as nano-crystals [11-12], graphene [13], Molecular Single Electron Transistors [14] and carbon nanotube [15]. Besides these materials, single aromatic hydrocarbons have gained much attention with regard to their application in molecular organic devices [16].

The use of individual molecules as functional electronic devices was first proposed in 1974 by Aviramet al [17], who proposed the idea of molecular diode for rectifying. The first single-molecule transistor was fabricated in 2000 [18], it was achieved using a single C_{60} molecule

---

bridging source and drain electrodes. In 2006, J. Tang et al was described the fabrication process of single molecule transistors using self-aligned lithography and in situ molecular assembly [19]. Using density Functional Theory (DFT) and the Non-Equilibrium Greens Functions (NEGF) technique, Parashara et al studied the electrostatic environment effect in molecular energy levels of single molecule transistors based on three polycyclic aromatic hydrocarbons (anthracene, tetracene and pentacene) [20]. In this respect, physical numerical simulations are of great help in describing and predicting molecular devices behavior.

In this paper, we studied the influence of different physical and electrical parameters on the I-V characteristic of a pentacene molecular transistor. Modeling two configurations "SMT" are highlighted. The first operates as a field effect transistor namely the molecular field effect transistor (MFET). The validation of the electrical characteristics was performed using MATLAB simulator, As a reference, we will compare our electrical characteristics results with those obtained from the numerical model of ref. [21]. We find significant gate-tuned the I-V features and further NDR behavior. Mechanisms are proposed, and the realization designs of five basic logic gates with only one single molecular FET (MFET) are also available. The second SMT configuration operates as a Molecular Single Electron Transistor (MSET). We have also investigated the electrical properties of this device using Atomistix ToolKit (ATK) a set of atomic-scale simulators, which can estimate properties of nano-scale devices. We discovered the additive properties in the I-V characteristics of MFET and MSET such as negative differential resistance (NDR) behavior, the dependence of the coulomb Staircase state and the various induced defects. These exciting electronic properties were acquired propagation interest because of prospective applications in future nano-electronic devices.

2. The single molecule transistors

Pentacene $C_{22}H_{14}$ is one of the most encouraging materials grown dramatically in recent years, as it offers better reliability [18], exceptional high charge carrier mobility [19], stability and a good on–off ratio [20]. It consists of polycyclic aromatic hydrocarbons with five fused benzene rings (Fig 1.a). In this section, we perform theoretical investigations of transport behavior in a single molecule transistor where the pentacene is covalently bonded to gold electrodes and used as an active semiconductor material. The structure used in our simulation is a single pentacene molecule with thiol (-SH) end groups bridging (Au) source and drain electrodes (Fig 1.b).The device channel length is 14.11 Å and width is 4.93 Å. The thiol groups are used to enhance the conductivity by modulating the contact work function. The Conduction of the molecule is modulated by a gate terminal electrode. HfO_2 ($\varepsilon_r = 25$) is used as a gate dielectric material with an a thickness equal to 5.5 Å [17].
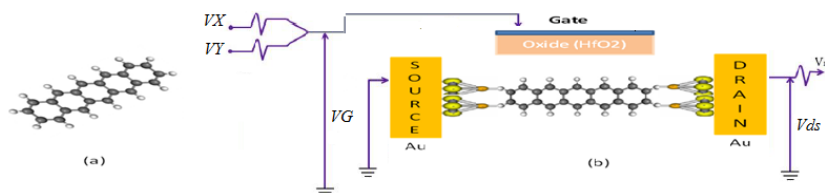

Fig. 1 (a) pentacene molecule, (b) Electric circuit diagram of a two-inputs (X and Y) logic gate incorporating one gated Single molecule transistor MFET (gray = carbon, white = hydrogen, orange =sulfur, yellow = gold).

The second structure was also simulation; it is consisted in a pentacene molecule setup in a SET geometry with a distance of 1.2 Å above dielectric as shown in the Fig 2. To the left and the right of the molecule, there are source-drain gold electrodes respectively. A metallic back-gate was used with 3.8 Å of dielectric material HfO_2 ($\varepsilon = 25$). The distance between the molecule and the electrode was kept 2.8 Å. Moreover, it was positioned at 1.2 Å above the dielectric.

We studied three types' defects in the pentacene molecule device:

i)   C-H$_2$ defect: created by adding one hydrogen atom to the C-H units so that the molecule turns on C$_{22}$H$_{15}$ (Fig 2.(b)).

ii)   C-O defect: Here we change hydrogen atom with oxygen one atom thus forming a double bond and making it fourfold coordinated (Fig 2.(c)).

iii)   C-O and C-H2 defects: Both C–H$_2$ and C-OH defects are present in the device which change the molecule into (C$_{22}$H$_{15}$O) (Fig 2.(d)). All defect configurations were optimized for the bond geometry and the relaxation to study their electronic transport properties.
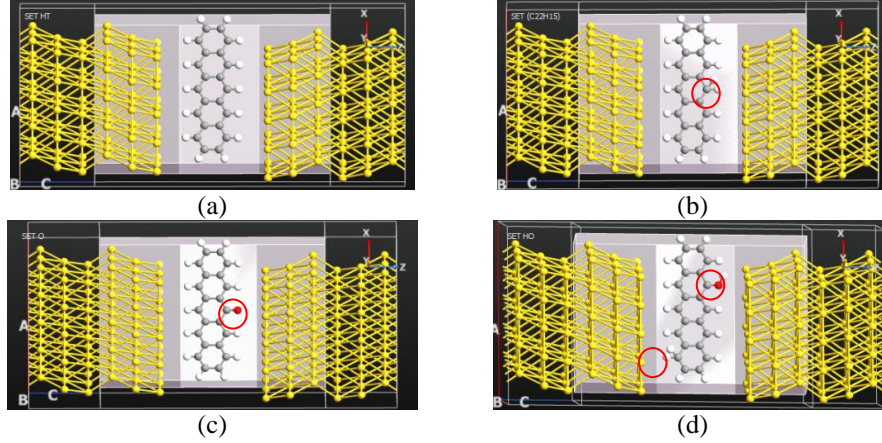

Fig. 2 MSET configurations (a) Stable device without defects (b) device with C–H$_2$ defect (C$_{22}$H$_{15}$) (c) device with C–O defect (C$_{22}$H$_{13}$O) (d) device with C–H$_2$ and C-OH defect (C$_{22}$H$_{15}$O) (oxygen =red).

3. Charge transport and computational methods

To describe charge transport in molecular field effect transistor (MFET), one needs to account for the fact that the number of electrons changes. In equilibrium condition, no current flows. The Fermi energy is typically positioned in the gap between the Highest Occupied Molecular Orbital (HOMO) and the Lowest Unoccupied Molecular Orbital (LUMO). The electrochemical potential of the electrodes depends on the applied bias voltage, the Fermi energy in the source contact (μ_S) increase by (qV_D) relative to the Fermi level in the drain contact (μ_D). The molecule conducts when the bias is large enough, which signify that one or more of the molecular energy levels lay between μ_S and μ_D. The chemical potential of the electrodes is shifted according to the following expressions [22]:

$$\mu_S = \varepsilon_F - \frac{eV}{2} \tag{1}$$

$$\mu_D = \varepsilon_F + \frac{eV}{2}$$

The energy distribution of the electrons is described by the Fermi–Dirac distribution function:

$$f_\alpha(E) = \frac{1}{1 + exp\left(\frac{\varepsilon_F - \mu_\alpha}{K_B T}\right)} \tag{2}$$

Where ε_F is the Fermi energy, μ_α the chemical potential of reservoir α (α is either the source (S) or the drain (D)) and T is a positive temperature. The discrete energy level ε has been treated as

discrete level, ignoring the broadening $\Gamma = \Gamma_S + \Gamma_D$ that arises due to the coupling with the source and drain electrodes. To take into account the broadening, we may replace the discrete level with a Lorentzian density of states D(E) [23]:

$$D(E) = \frac{1}{2\pi} \frac{\Gamma}{(E - \varepsilon)^2 + \left(\frac{\Gamma}{2}\right)^2} \qquad (3)$$

To simulate our nano-transistor the DOS will be written as:

$$D_\varepsilon(E) = \frac{m*WL}{\pi h^2} \theta(E - E_c) \qquad (4)$$

Where E_C is the energy of the conduction band edge, m* is a particle's effective mass, W is the molecule channel width, L is the molecule channel length. The self-consistent potential is:

$$U_{SC} = U_L + \frac{q^2}{C_E}(N - N_0) \qquad (5)$$

Where U_L is the Laplace potential, N is the number of electrons and q is the charge of an electron:

$$U_L = \frac{C_G}{C_E}(-qV_G) + \frac{C_D}{C_E}(-qV_D) \qquad (6)$$

C_E is the total capacitance given by:

$$C_E = C_S + C_G + C_D \qquad (7)$$

The effect of the self-consistent potential U_{sc} is to increase the density of states (DOS) in energy to be used in our simulation. Consequently, the broadening effect can be include in the expression of the current I and the number of electrons N which will be given by:

$$N = 2 \int_{-\infty}^{+\infty} dED(E) \frac{\Gamma_S f_S(E) + \Gamma_D f_D(E)}{\Gamma} \qquad (8)$$

$$I = \frac{2q}{h} \int dE 2\pi D_\varepsilon(E - Usc) \frac{\Gamma_S \Gamma_D}{\Gamma_S + \Gamma_D} \left[f_D(E - \mu_D) - f_S(E - \mu_S) \right] \qquad (9)$$

We write in this form:

$$I = \frac{2q}{h} \int dE \overline{T}(E - Usc) \left[f_D(\varepsilon - \mu_D) - f_S(\varepsilon - \mu_S) \right] \qquad (10)$$

Where $\overline{T}$ is the transmission function and it is defined according to the following equation:

$$\overline{T}(E) = 2\pi D_\varepsilon(E) \frac{\Gamma_S \Gamma_D}{\Gamma_S + \Gamma_D} = \frac{\Gamma_S \Gamma_D}{(E-\varepsilon)^2 + (\Gamma/2)^2} \qquad (11)$$

We have implemented the current's expression described above in MATLAB simulator. In our model, the first step was defining the constant parameters which are the molecular intrinsic constants, the device operating conditions, the molecular charging energy, the coupling conditions with the micro scale regions inside the transistor as well as the condition for equilibrium through the device. The next step was defining the bias conditions, it was important to insure that the real voltage range for transistor operation corresponded to the low voltage range. Then, to characterize the molecule properties, we used a simple semi-empirical Hamiltonian H and a self-consistent potential U_{SC}. Using self-energy functions Σ_S and Σ_D to describe the effect of the source and drain contacts, we defined the Fermi levels to identify the electrodes. When the electron density ρ is calculated, we solve the Poisson's equation to get the self-consistent potential U_{SC}. A flow diagram represents the algorithm used in MATLAB and a schematic view of the simulated device is shown in Fig 3.

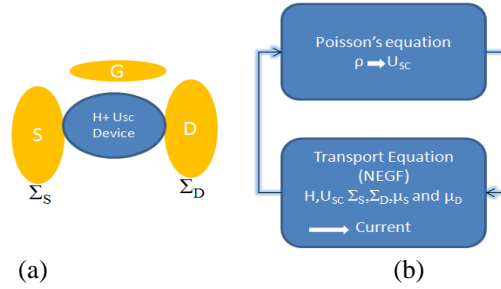(a)   (b)

Fig. 3 (a) Schematic view of a molecule coupled to source and drain contacts,
(b) description of the flow process based on self-consistent calculation
and NEGF transport Equation

In this section, we presented the modeling of the Molecular Single Electron Transistor (MSET) (fig 4) and we studied the defect effects on its electrical performance, we used Atomistic ToolKit (ATK) simulator, which is based on the combined the DFT theories and the NEGF formalism [24][25]. Such simulations are used to model the electronic and physical properties of molecules, crystals, and molecular devices using both non-self-consistent tight-binding models and a self-consistent. In particular, our proposed model is used to study the electron transport through an organic molecule between gold surfaces. The electrode Poisson solver calculations are carried out with boundary conditions as periodic and the Brillouin zone integration is carried out with 1x10x100 k-point sampling. The electron temperature is taken as 300 K. For computing electrostatic potentials, we have utilized a real space grid, with mesh cutoff energy equal to 75 Hartree. The source and drain electrodes are extracted along (111) direction of bulk gold. The optimization of the total energy of the overall geometry configuration give a fixe distance between the electrodes. The large supercell dimension is taken in the perpendicular direction of electron transport there is no interaction or less between the pentacene molecule and their mirror. Also, we used as 24A° the size of the supercell in the y-direction. The I-V characteristics flowing between the source and drain electrode is given by the following formula:

$$I_{S-D} = \frac{2e}{h} \int T(E, V_{S-D})[f(E-\mu_S) - f(E-\mu_D) \,\mathrm{d}E \qquad (12)$$

4. Simulations results

At the molecular scale, there is a many experimental techniques that have been industrialized to fabricate single molecule devices including mechanical break junctions, scanning probe microscopy (SPM), mechanically controlled break junctions (MCBJs) [26] , electrochemical deposition [27], electro-migration break junctions (EBJs) [23-24] and Self-assembly of nanostructures [30]. The current in these devices is generally affected by many factors such as the position of the Fermi level in the metal–molecule–metal junction through the thiol group (i.e Se, S), the nature of the molecular bridge, the contacts, the strength of the molecule-electrode interaction, and the electronic properties of the molecule. Many phenomena can be adapted by the choice of the molecule or the suitable separation between the thiolated molecule ends and the contacts.

4.1. Molecular Field Effect Transistor MFET

In this section, we present the influence of the bias voltage on the I-V characteristics using Matlab simulator. The existence of electronic channels in the molecule is highly dependent on the load that enables and disables charge transport under a bias. When the charge is zero, there is neither LUMO transport between the two terminals of the molecules, nor conduction channels. However, as the voltage increases, the molecule becomes more charged, the LUMO orbital extends over the two ends of the molecule and the electronic pathways connect the electrodes, thereby maximizing electron transport. Thus, the transport properties depend much more on the coupling effect between pentacene and the gold electrodes. We observe that some bias values produce nonlinear transport phenomena, implying NDR for a pentacene molecular junction. The negative differential resistance behavior is expected when sharp transmitting states of such molecular junctions are resonantly shifted under a bias.

Generally, the strong field effect in the conductance for an applied voltage give a current modulation by changing the polarity of a gate field. Varying the gate voltage, change the Fermi level of the molecule. As a consequence, some of the transmission modes close to the Fermi level will be suppressed. Which affect the current flow between source and drain. This gives us a non-linear current resulting the NDR.
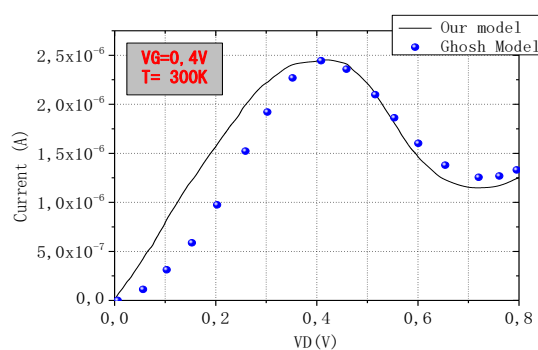

Fig. 4 MFET I-V curves, (in black) our model, (in blue) the B. Ghosh model @T=300 K and VG = 0 .4 V.

Fig 4 show the output characteristics of the simulated MFET device. Our result show a good agreement with those of the *I-V* curve presented in ref [21]. These results give us the possibility of establishing FETs based on molecular devices. For different gate biases, the linearity of current increases rapidly at low voltage, showing the gate voltage can improve and control the transport properties, and change the system from semiconducting to metallic.
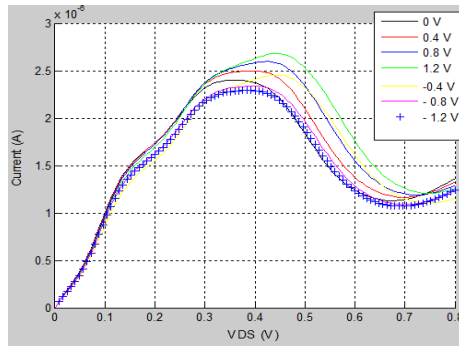
Fig. 5 The I–V characteristics of the MFET with different source drain voltages (V_G) @T=300 K.

As we can see, no matter whether V_G is applied, NDR behaviors are modulated. So, this opens up the door to realize a low consumption circuits as gate logic. Here we present an advance to see five basic logic gates with single pentacene molecular FET at $V_{DS} = 0.75$ V, which is similar to the design scheme proposed by R. Hariharan et al [31]. The electric circuit diagram is shown in the Fig. 1. We present calculated source drain resistance as a function of V_G at $V_{DS} = 0.75$ V as shown in Fig. 6.
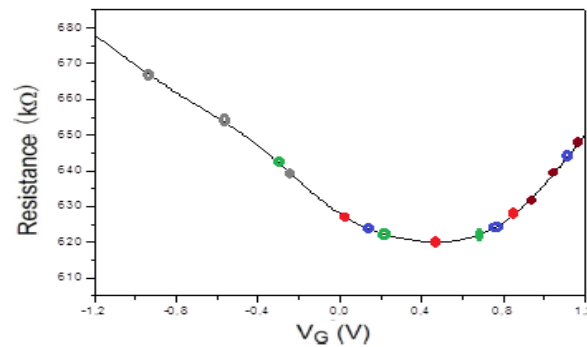

Fig.6 Source-drain resistance (R) curve versus V_G at $V_{DS} = 0.75$ V

We put V_G as an arithmetic average of the two inputs VX and VY, ie, Vg = (VX + VY) / 2. The two digital inputs VX and VX both have two values: high V1 (Boolean 1) and low V0 (Boolean 0) and therefore, V_G have three possible values: V0 (both inputs 0), V1 (both inputs 1) and Vr = (V0+V1)/2 (different inputs). If the voltage levels V0 and V1 are selected such that the minimum of the curve is to V_G = Vr and has an identical higher value to V_G = V0 or V1 (these three operating points are designated by red color of Figure 6, the resistance R is low (0) for different inputs and high (1) when both inputs are the same, the XNOR gate is obtained. Also, if the voltage levels are chosen such that the resistance R is low for V_G = V0 or Vr and high for V_G = V1, the AND gate is obtained. Similarly, if the resistance R is high for V_G = V0 and low for V_G = Vr or V1, the NOR gate is obtained. Finally, a NOTX gate is obtained if R (V_G=V1) < R (V_G=Vr) <R (V_G=V0) On the other hand, if R(V_G=V1) > R(V_G=Vr) >R(V_G=V0) a YESX gate is obtained. The truth table of all logic gates is given in the table.1.

Table 1 The truth table of all logic gates.

VX	VY	o XNOR	o NOR	o AND	o NOT X	o Yes X
0	0	1	1	0	1	0
0	1	0	0	0	X	X
1	0	0	0	0	X	X
1	1	1	0	1	0	1

To further understand the performance of all logic gate, we look at three equidistant operating points (marked by color) correspond to different uses of the logic gates as shown in Figure 7. An XNOR gate (red) is obtained for Vr (Vg of the middle point) =0.45V and V_G (total gate voltage swing) = 0.9V, a NOR gate (green) for Vr = 0.21V and V_G = 1V, an AND gate (bleu) for Vr = 0.8V and V_G = 0.95V, a NOT gate (gray) for Vr = 0.57V and V_G = 1.12V.

The designing of a single molecular FET used to realize five basic logic gates with just one MFET offer a promising alternative to conventional gates due to their minimum transistors number   and small size In addition, we note that this component has small size and a low consumption compared with molecular gate logic in the literature [31].

Generally, SET and FET characteristics are very different. The electrostatic effect is one common thing in both of these two devices, but in the SETs case, the Coulomb blockade effect makes the electrons not free to move from source to drain [32]. An electron approaching a small negative charged region experiences the electrostatic repulsion by the previous electron in that region. This regulates the number of electrons one-by-one in the channel. We propose to study the electrical characteristics of pentacene based SET device called "MSET".

4.2. Molecular Single Electron Transistor

For the First time, we have studied the electrical properties of Molecular Single Electron Transistor based on single pentacene molecule. In MSET simulation cases, the applied gate voltage is taken 0.4 V while the drain voltage is taken over a range of 0 - 4 V.
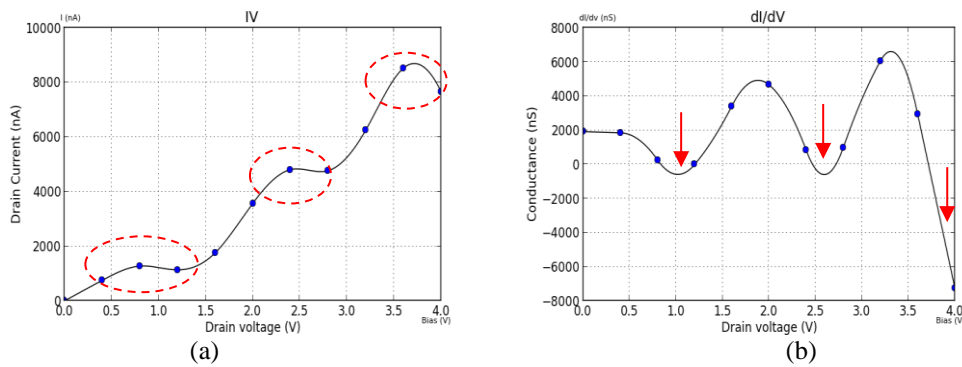

Fig.7 (a) The I–V characteristics of the device without (V_G = 0.4 V).
(b) The Conductance of the device without defect (V_G = 0.4V).

In fig 7.(a), we present the *I–V* characteristic of the stable MSET device (without defects). The curve clearly displays the coulomb Staircase state and NDR behavior which depends on the Coulomb interaction between electrons. Also, we show the presence of three current peaks, which lies at 0.84V, 2.47 V and 3.73 V and these values of the current are 279 nA, 4843 nA and 8696 nA respectively. The negative values of the conductance clearly confirm the three peaks as shown in fig 7.(b). The corresponding PVR windows are 145 nA, 110 nA, 1031 nA, respectively.

To get a better understanding of the relationship between the electronic structure and the transport properties of the molecular device, we consider the study of three types defects in the pentacene molecule device described above. The effects of various oxygen- and hydrogen-induced

defects can adjust the NDR behavior which give different area where this behavior NDR is presented. This last, can be used for designs of different logic gates according to the applied VDS voltage range.
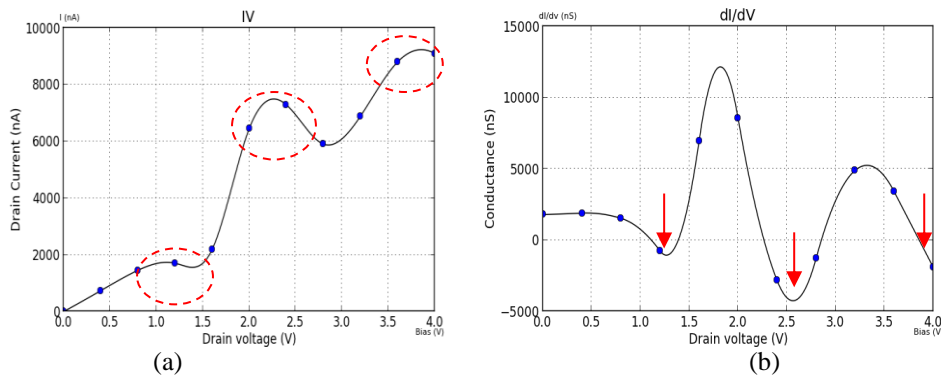

Fig. 8 (a) The I–V characteristics of the device with C–H_2 defect ($C_{22}H_{15}$)) (V_G = 0.4 V).
(b) The Conductance of the device with C–H_2 defect (V_G = 0.4 V)

By adding one hydrogen atom to the C-H units as a defect, the *I-V* characteristics get affected as shown in fig 8.(a). The H atom acts as a barrier, and the electronic transport occurs via a resonant tunneling mechanism. The influence of Coulomb interaction is clearly seen   to be increasing the NDR region. As the plot shows, the NDR regions can be seen to start from these points (1.12 V, 2.27 V, and 3.86V) onwards with a PVR window of 170 nA, 1625 nA and 136 nA respectively. In the fig 8.(b) we show the conductance curve, which attains a maximum of 2100 nA at a bias voltage of about 0.33 V. In addition, the negative value of the conductance which correspond the NDR behavior.
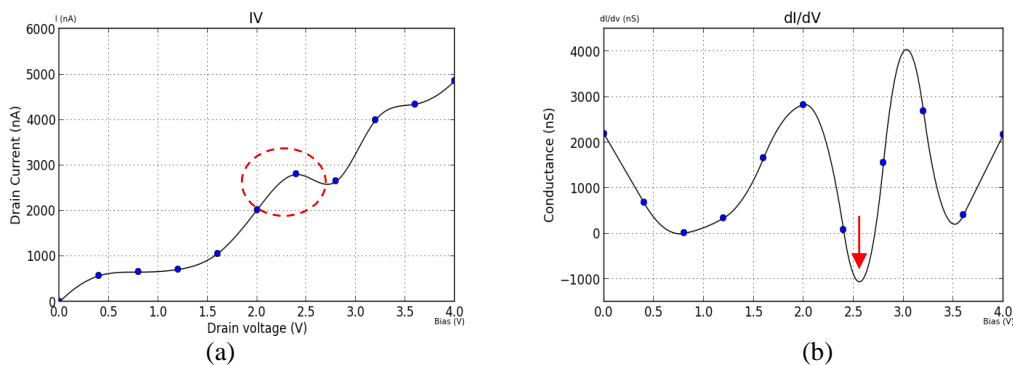

Fig. 9 (a) The I–V characteristics of the device with C–O defect ($C_{22}H_{13}O$) (V_G = 0.4 V).
(b)The Conductance of the device with C-O defect (V_G = 0.4 V)

Next, we present the effect of C-O defect in the performance of MSET. In Fig 9.(a), the influence of this defect on the I–V characteristic of the device is shown. In this case, the curve shows a rising edge at zero bias voltage. The channel current increases till it achieves a maximum at 2.41 V bias voltages with the corresponding current of 2800 nA after which it decreases further right being 2583nA at 2.72 V. There is only one NDR region that can be seen starting from this point (2.41 V) with a PVR window 217 nA. The negative conductance values (negative differential conductance NDC) represent the NDR behavior corresponds to the *I-V* characteristic. Fig 10.(a) shows the *I–V* characteristic of MSET with C–H2 and C–OH defects. As can be seen from the plots, the channel current shows a rising edge at zero bias voltage. In this case, the characteristic of the MSET is representing coulomb Staircase state without NDR effect at low

voltage. We should increase the source drain voltage to see the NDR effect. The maximum current is achieved at a bias voltage of 3.7 V, of magnitude 1651 nA with a PVR window 181 nA.
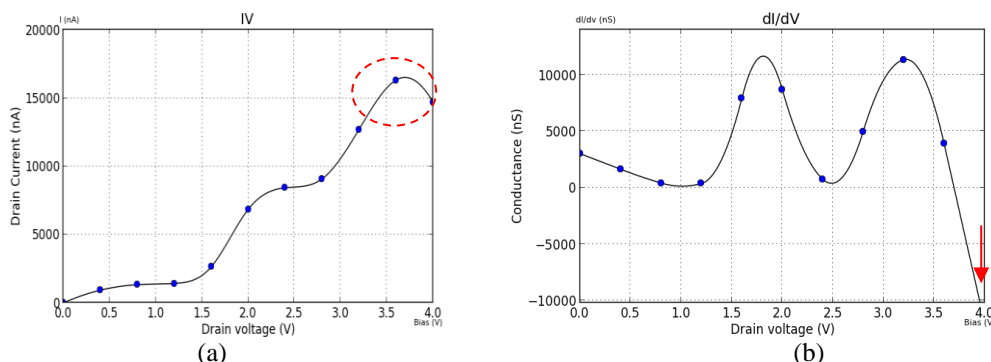

(a)
(b)

Fig. 10 (a) The I–V characteristics of device with C–H$_2$ and C-OH defect (C$_{22}$H$_{15}$O) (V$_G$ = 0.4 V).
(b) The Conductance of the device with C–H$_2$ and C-OH defect (V$_G$ = 0.4 V)

The conductance characteristic of the device with C–H$_2$ and C–OH defects plot is shown in fig 10.(b), in which the conductance is seen with coulomb oscillations. The NDR effect presented from the conductance curves at 3.7V when the conductance has a negative value. The absence of the NDR effect at low bias voltage confirmed that the electronic property of a molecule has been affected by the presence of the two types of defects. The transmission spectra corresponding to four cases are shown in fig 11.(d).
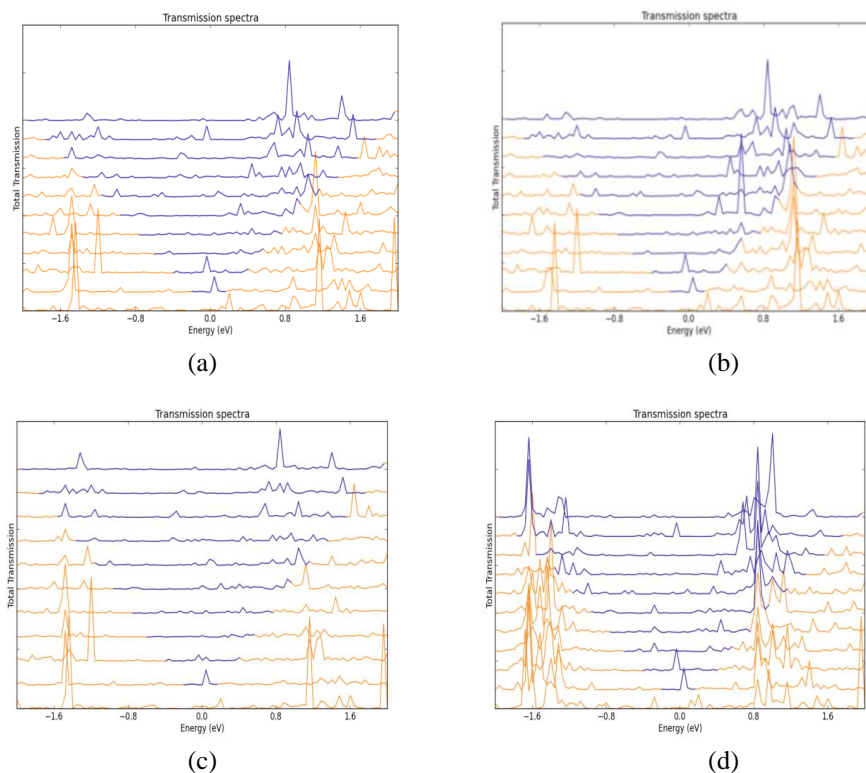

(a)
(b)

(c)
(d)

Fig. 11. Transmission spectra corresponding to all the four cases: (a) normal device with no defect (b) device (C$_{22}$H$_{15}$) with C–H$_2$defect. (c) device (C$_{22}$H$_{13}$O) with C–O defect (d) device (C$_{22}$H$_{15}$O) with C–H2 and C-OH defect.

This NDR behavior can be explained also by the transmission spectra of the device configuration which is presented in Fig 11. As the drain bias is increased, some of the transmission

modes close to the Fermi level seem to be suppressed. We note that, if the reduction in transmission is rapid enough to exceed the increased Fermi window, when the bias voltage increases, the current has a negative slope, which leads to the NDR behavior. In addition, the LUMO becomes completely delocalized allowing improved conduction, thus creating the appearance of the NDR peak. When the bias voltage increases, the molecule becomes doubly reduced, the LUMO becomes localized across the molecule and decreases the molecular conductivity, which reduces the current. The NDR effect observed in the I-V curve is caused by tunneling through discrete quantum-mechanical states and a small density of states (DOS) of the molecular levels. The electron tunneling from the molecule decreases from one electrode to the other. This tunneling causes a decrease in the transmission resonance peaks.

5. Conclusions

In this paper, a Single molecule transistor based pentacene has been simulated using MATLAB simulator. The MFET I-V curves were performed using density functional theory (DFT) model in conjugation with the non-equilibrium green's function (NEGF) formalism. Our simulation shows good agreement with those obtained in the literature and the theoretical results specify that the currents can be effectively tuned by the gate bias V_G. The NDR behaviors, which are observed nearly at the same V_{DS} bias. We show the application of using one gated molecular device to realize five basic logic gates with small size and a low consumption. We have also studied the electrical properties of a pentacene-based Single Electron Transistor (MSET) using Atomistix ToolKit (ATK).

We find that the simulated device operates as a Single electron transistor with conduction based on the Coulomb blockade phenomenon allowing the transit of electrons sequentially. We have also presented the effect of the various induced defects on the MSET the I–V characteristics, conductance and transmission spectrum. We found that these defects have a strong influence on the electron transport properties and especially on the NDR effects. This behavior could be highly useful in the miniaturization of various circuits such as memory cells, amplifiers, gate logic and RF oscillators. Our calculations also indicate that pentacene molecule can be used as low bias NDR device, which provide promising route for the applications in the field of molecular electronics with stability and low power dissipation in the future.

References

[1] F. Molina-Lopez, R. E. de Araújo, M. Jarrier, J. Courbat, D. Briand, and N. F. de Rooij, Microelectron. Reliab. **54**(11), 2542 (2014).

[2] D. Qin, M. Wang, Y. Chen, L. Chen, G. Li, Phys. Scr., **89**(1), 15802 (2014).

[3] S. Yamada, C.-H. Shim, T. Edura, A. Okada, C. Adachi, S. Shoji, J. Mizuno, Microelectron. Eng. **161**, 94 (2016).

[4] S. Dimitrov, B. Schroeder, C. Nielsen, H. Bronstein, Z. Fei, I. McCulloch, M. Heeney, J. Durrant, Polymers (Basel). **8**(1), 14 (2016).

[5] Ö. A. Yokuş, F. Kardaş, O. Akyıldırım, T. Eren, N. Atar, M. L. Yola, Sensors Actuators B Chem. **233**, 47 (2016).

[6] S. B. Aziz, J. Electron. Mater. **45**(1), 736 (2016).

[7] R. M. Hariharan, D. J. Thiruvadigal, Nanosyst. Physics, Chem. Math. **4**(2), 294 (2013).

[8] Y. Xu, C. Fang, B. Cui, G. Ji, Y. Zhai, D. Liu, Appl. Phys. Lett. **99**(4), 129 (2011).

[9] R. R. Nejm, A. I. Ayesh, D. A. Zeze, A. Sleiman, M. F. Mabrook, A. Al-Ghaferi, M. Hussein, J. Electron. Mater. **44**(8), 2835 (2015).

[10] K. Gao, L. Xiao, Y. Kan, B. Yang, J. Peng, Y. Cao, F. Liu, T. P. Russell, X. Peng, J. Mater. Chem. C **4**(17), 3843 (2016).

[11] S. Wang, G. Yang, and S. Yang, J. Phys. Chem. C, **120**(1), 802 (2016).

[12] T. Hasegawa, J. Takeya, Sci. Technol. Adv. Mater. **10**(2), 24314 (2009).

[13] B. Hafsi, A. Boubaker, N. Ismaïl, A. Kalboussi, K. Lmimouni, J. Korean Phys. Soc.

67(7), 1201 (2015).

[14] A. Srivastava, B. Santhibhushan, V. Sharma, K. Kaur, M. Shahzad Khan, M. Marathe, A. De Sarkar, M. Shahid Khan, J. Electron. Mater. **45**(4), 2233 (2016).

[15] C. X. Zhang, E. X. Zhang, D. M. Fleetwood, M. L. Alles, R. D. Schrimpf, C. Rutherglen, K. Galatsis, Microelectron. Reliab., **54**(11), 2355 (2014).

[16] L. Torsi, "Microelectron. Reliab. **40**(4–5), 779 (2000).

[17] A. Aviram, M. A. Ratner, Chem. Phys. Lett. **29**(2), 277 (1974).

[18] P. L. McEuen, H. Park, J. Park, A. K. L. Lim, E. H. Anderson, A. P. Alivisatos, Nature, **407**(6800), 57 (2000).

[19] J. Tang, E. P. De Poortere, J. E. Klare, C. Nuckolls, S. J. Wind, Microelectron. Eng., **83**(4–9), 1706 (2006).

[20] S. Parashar, P. Srivastava, M. Pattanaik, IOP Conf. Ser. Mater. Sci. Eng., **73**, 12117 (2015).

[21] B. Ghosh, A. Gramin, J. Theor. Appl. Phys. **9**(3), 213 (2015).

[22] M. L. Perrin, E. Burzurí, H. S. J. van der Zant, Chem. Soc. Rev. **44**(4), 902 (2015).

[23] D. Hien, H. Trung, J. Phys. Conf. Ser. **1876**, 12087 (2009).

[24] M. Brandbyge, J.-L. Mozos, P. Ordejón, J. Taylor, K. Stokbro, Phys. Rev. B **65**(16), 165401 (2002).

[25] "Atomistix Virtual Nanolab, QuantumWiseInc."

[26] Y. Kim, H. Song, J. Nanosci. Nanotechnol. **15**(2), 921 (2015).

[27] Y. Yang, J. Liu, S. Feng, H. Wen, J. Tian, J. Zheng, B. Schöllhorn, C. Amatore, Z. Chen, Z. Tian, Nano Res. **9**(2), 560 (2016).

[28] L. Sun, Y. A. Diaz-Fernandez, T. A. Gschneidtner, F. Westerlund, S. Lara-Avila, K. Moth-Poulsen, Chem. Soc. Rev., **43**(21), 7378 (2014).

[29] D. Xiang, X. Wang, C. Jia, T. Lee, and X. Guo, Chem. Rev. **116**(7), 4318 (2016).

[30] J. Wen, W. Li, S. Chen, J. Ma, Phys. Chem. Chem. Phys. **18**(33), 22757 (2016).

[31] R. M. Hariharan, D. J. Thiruvadigal, "MODELLING LOGIC GATES DESIGN USING PYRROLE BASED SINGLE MOLECULAR FIELD EFFECT TRANSISTOR," **11**(3), 873 (2016)

[32] A. Boubaker, M. Troudi, N. Sghaier, A. Souifi, N. Baboux, A. Kalboussi, Microelectronics J., **40**(3), 543 (2009).